

0017-9310(94)00314-9

# Isokinetic sampling probe and image processing system for droplet size measurement in two-phase flow

G. J. ZHANG† and M. ISHII‡

School of Nuclear Engineering, Purdue University, West Lafayette, IN 47907, U.S.A.

(Received 5 April 1994 and in final form 23 September 1994)

**Abstract**—The present system consists of an isokinetic sampling probe, droplet collection mechanism and an image processing package. A droplet sample was extracted from flow field by the sampling probe and collected by an immiscible liquid. Droplet images were grabbed and digitized by an image processing system. Image processing software was developed for droplet counting and sizing, with the capability of distinguishing overlapping droplets. Possible measurement distortion factors such as droplet deposition in the probe, droplet breakup and coalescence were studied. A simple criterion for minimizing measurement distortion was obtained. The system can be used for both water and liquid-metal droplets.

## 1. INTRODUCTION

An accurate knowledge of droplet size distribution is important in studying mass, momentum and energy transfer in dispersed two-phase flow. Various techniques have been developed for the measurement of droplet sizes. The development of the present system for droplet size measurement was motivated by the study of droplet dispersion phenomenon in the Direct Containment Heating (DCH) scenario [1] in severe nuclear reactor accidents. The DCH problem starts after a reactor core meltdown event. Due to the high temperature and large mass of molten core materials (corium), the bottom wall of the reactor vessel may be melted through. The failure of the reactor vessel results in a discharge of corium and the blow-down of steam from the high-pressure primary system into the reactor cavity. Part of the corium will be atomized into small droplets by the high-velocity steam and some droplets may disperse into the reactor containment. Heat transfer from corium, heat generation due to the oxidation of metallic materials, a possible hydrogen combustion and the heat and mass addition from the blow-down steam may lead to considerable pressurization of the reactor containment. The containment integrity is then threatened. The failure of the containment will cause the release of radioactive materials into the atmosphere. In this so-called Direct Containment Heating (DCH) scenario, droplet sizes and the degree of dispersion are the crucial factors governing the rates of heat transfer and chemical reaction. If the droplet size is small and the degree of droplet dispersion is high, the risk to the containment

can be high. In order to assess the containment performance in such an accident, a simulated DCH experiment was planned to study corium entrainment and dispersion. Two kinds of fluids, water and liquid metal, will be used to simulate the corium in the experiment.

Unlike other two-phase systems, DCH experimental conditions, such as the transient flow, high droplet mass flux, liquid film on the wall and the use of liquid metal, make all conventional drop size measurement techniques difficult to apply [2, 3]. First, DCH is a fast transient process and lasts only few seconds, therefore, methods that require steady operating conditions, such as the electrical needle method [4], are not applicable. Secondly, in both air–water and air–liquid metal simulation experiments, liquid flow rates are extremely high so that all the walls of the test section will be covered by thick liquid films. In the liquid metal case, the test section becomes completely non-transparent. Although optical methods and photographic methods are well developed, non-transparency conditions rule out their applicability. The difficulty in finding a satisfactory method has led us to the development of the present system for droplet size measurement.

The primary objective of the research was to develop a droplet size measurement system that can be used under the difficult DCH conditions, but it can also be used for other droplet flow situations. In the course of developing the system, concerns about the effects of droplet deposition inside the probe, droplet breakup and coalescence during the collection on measurement distortion were raised. These problems were studied and practical solutions were provided. A simple criterion for minimizing the distortion factors was obtained. The system can measure droplet diam-

† Current address: Exxon Production Research Company, P.O. Box 2189, Houston, TX 77252, U.S.A.

‡ Author to whom correspondence should be addressed.

### NOMENCLATURE

$D$	droplet diameter	Greek symbols	
$j$	volumetric flux	$\mu$	viscosity
$k$	ratio of characteristic diameters	$\xi$	distribution parameter
$P$	total pressure	$\rho$	density
$p_s$	static pressure at the tip of sampling probe	$\sigma$	surface tension.
$p_\infty$	pre-existing static pressure at the tip of sampling probe	Subscripts	
$Re$	Reynolds number	f	liquid
$u$	velocity	g	gas
$v$	volumetric fraction of droplets	max	maximum droplet diameter
$y$	logarithmic value of dimensionless diameter.	s	sampling point
		vm	volume median diameter
		32	Sauter mean diameter.

eters from 10  $\mu\text{m}$  to 3 mm, and it is suitable for both water and liquid-metal droplets.

## 2. SYSTEM COMPONENTS AND OPERATION

### 2.1. Experimental setup

The present droplet size measurement system consists of three major parts, an isokinetic sampling probe, a droplet collection box and an image processing system. Figure 1 shows the experimental set-up for droplet generation and droplet sampling. The horizontal test section is a 1.83 m long lexan tube with an inside diameter of 2.5 cm. Liquid (water or liquid-metal) was injected through a 1.6 mm (i.d.) nozzle from the liquid discharge tank. When the nozzle was located at the center of the flow channel, droplets were generated by liquid-jet disintegration. When the nozzle was lowered to the wall, liquid films were first formed and droplets were then produced by entrainment. A low melting temperature alloy, woods-metal (melting temperature of 70°C), was used for liquid-metal droplet

generation. Electric heaters were used to pre-heat the flowing gas and the whole test section to temperatures above the melting temperature of the alloy so that the woods-metal remained liquid within the test section.

An isokinetic sampling probe was mounted parallel to the stream-line at the elbow of the test section and connected to a droplet collection box. The collection box was connected to the expansion section which was located down-stream of the test section. The pressure at this section was much lower than that at the tip of the probe. By adjusting the sampling valve, the pressure in the collection box was controlled, and so was the sampling rate. The sampling rate was controlled such that an isokinetic sampling condition was established at the tip of the probe. Under the isokinetic condition, the static pressures inside and outside the probe are equal, thus, the sampling rate is exactly same as that before the insertion of the sampling probe. Anisokinetic sampling may result in a surfeit or a deficit of small droplets due to over-suction or under-suction of gas.

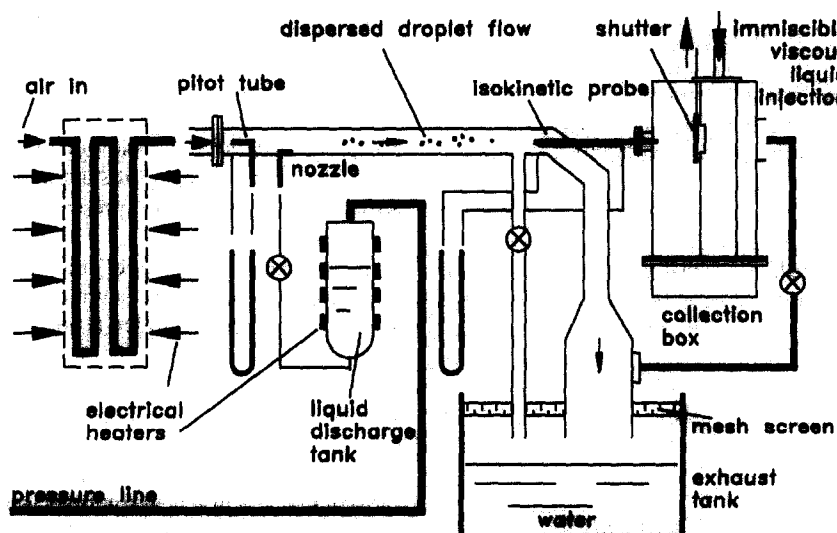


Fig. 1. Experimental set-up for droplet generation and droplet sampling.

After a sample of droplets were taken from the flow field, the sampled droplets were captured by an immiscible liquid in a specially designed droplet collection box. Different collecting liquids and collection methods were used for different liquid droplets. After the collected droplets settled down in the collection liquid, an image processing system was used for droplet counting and sizing. Finally, a size distribution was obtained for a sample of droplets.

## 2.2. Isokinetic sampling probe

Isokinetic sampling probes have been widely used for velocity or mass flux measurements in single-phase and two-phase flows [5] as well as in solid particle sampling and size measurement [6]. However, its application to droplet sampling and size measurement has not been explored due to the difficulties of droplet collection and possible measurement distortion caused by droplet deposition, breakup and coalescence.

The isokinetic probe consists of two thin-wall tubes, the larger sampling tube and the smaller pressure tube (see Fig. 2). For velocity or mass flux measurement, the sampling tube usually has an inside diameter smaller than 1.0 mm. For droplet sampling, larger sampling tubes (4.7 mm, 7.9 mm and 11.1 mm) were used in order to reduce droplet deposition inside the probe. For incompressible single-phase flow, fluid velocity is related to the dynamic pressure by a simple relationship

$$\frac{1}{2}\rho u_{\infty}^2 = P - p_{\infty}. \quad (1)$$

A similar but more complicated relationship can be obtained for two-phase flow [7, 8]. According to equation (1), any disturbance in the pre-existing local pressure will lead to the deviation in the measured velocity. If the velocity deviation is small, such an error in the measurement can be easily derived from equation (1) as

$$\frac{u_s - u_{\infty}}{u_{\infty}} = -\frac{p_s - p_{\infty}}{\rho u_{\infty}^2}. \quad (2)$$

On the other hand, if an isokinetic condition ( $p_s = p_{\infty}$ ) is reached, the measured velocity will be equal to that of undisturbed steam. An isokinetic condition is essential for a correct velocity measurement. Especially in

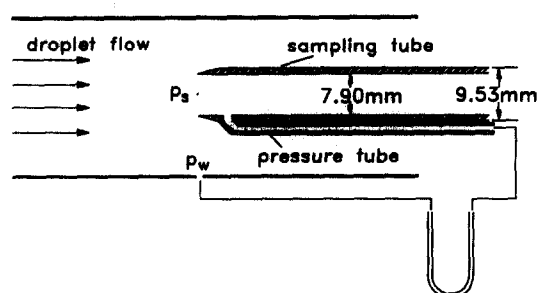


Fig. 2. Configuration of an isokinetic sampling probe.

a two-phase system, a slight deviation from the isokinetic condition can cause an appreciable error in the gas velocity measurement. For droplet sampling, the gas velocity is not our direct concern. However, over-suction or under-suction of gas will result in a surfeit or deficit of small droplets. Some empirical correlations were developed for anisokinetic sampling correction [6]. If the deviation is small, however, the change of gas stream occurs only within a very short distance from the probe tip. Unless the sizes of droplets are extremely small (sub  $\mu\text{m}$  range), the motion of most droplets will not be affected due to the large inertia of droplets. Hence, if the error in the mean gas velocity is about the same order with the turbulence level, the anisokinetic sampling condition is not expected to affect the droplet size measurement. A similar conclusion was given by Paras *et al.* [9]. Therefore, it can be concluded that the operation of the isokinetic probe is much easier for droplet sampling than for the velocity measurement.

## 2.3. Methods for droplet collection

It is not an easy task to collect high-velocity droplets without causing the change of their sizes. Careful measures must be taken to prevent droplet breakup and coalescence during the collection process. One of the oldest methods was to expose an oil-coated plate to the droplet flow. But the thin layer of oil film on the plate may not be sufficient to prevent breakup of large droplets and coalescence of droplets. Another method was to freeze droplets using a cold gas, but it required a long freezing distance, which made the system large and complicated. Rao [10] developed a method of using liquid nitrogen injection to freeze drops inside the probe. The drawback of this method was that the frozen droplets and film might block the probe.

In the present system, two different methods were developed for collecting droplets. Figure 3(a) shows the method of using a falling oil film to collect water droplets. Viscous oil was injected into the collection chamber in the box to form a falling oil film. Incoming droplets were captured in the oil film and transported to a portable container. Since the clean oil was supplied continuously, the problem of droplet coalescence encountered in the oil-plate technique could be essentially eliminated. In the course of studying droplet collection, it was found that, if the collection liquid had a high viscosity, a smaller surface tension and a slightly smaller density than those of droplets, the droplet could be stopped within a short distance from the surface in the liquid without disintegration. The penetration distance was as short as several droplet diameters. This method is simple and effective for low density droplets. The droplet and collecting liquid must be immiscible, such as the water drops and oil film.

For heavier liquid-metal droplets, a pool of liquid was used for droplet collection because liquid-metal droplets have a much longer penetrating distance due to their large inertia. Figure 3(b) shows the method

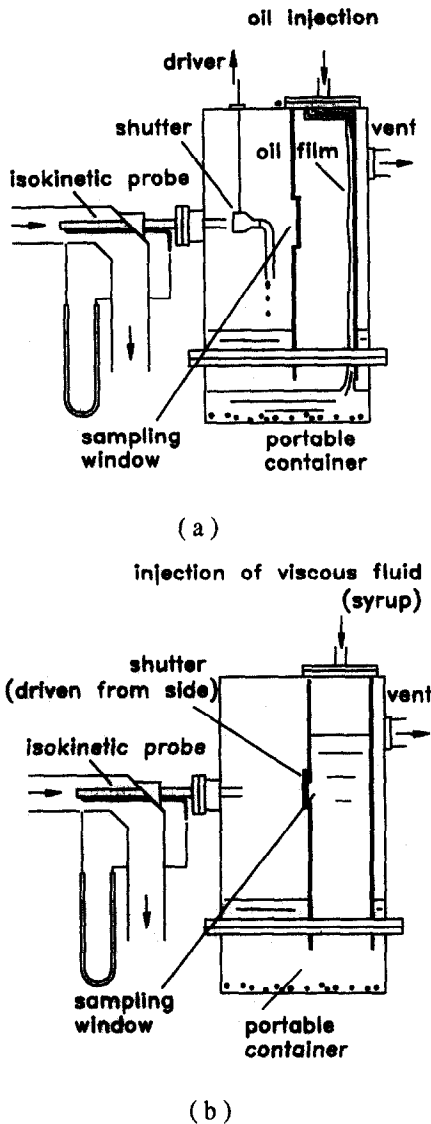


Fig. 3. (a) Falling oil film method for water droplet collection; (b) liquid pool method for liquid-metal droplet collection.

used for woods-metal droplet collection. In order to effectively stop the liquid-metal droplets, viscous syrup was used as a collection liquid. The syrup was made by melting five parts (of mass) of pure granulated sugar and mixing with one part (of mass) of water. The syrup was injected into the pool to a level above the sampling window. The shutter opened up when sampling began. Due to the gas impact pressure on the window area, the syrup did not flow out of the pool, thus the liquid level was maintained. After woods-metal droplets penetrated into the pool, they were stopped in the syrup and then solidified. It was found in the experiment that frozen droplets could be in nearly spherical shape or in irregular shape, depending on the temperature difference between droplets and the collection liquid. It was considered important to keep the collection fluid temperature

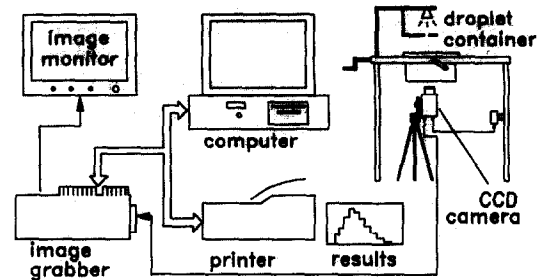


Fig. 4. Image processing system for analyzing droplet sizes.

close to the freezing temperature of droplets. When the temperature of the collection fluid was well below the droplet freezing temperature, the droplets deformed and some breakup took place at the impact due to the high surface tension gradient caused by the thermal gradient. Between the probe and collection chamber, an electric shutter was installed to control the interval of sampling time. With this, the droplet number density in a sample can be controlled low enough not to cause coalescence.

#### 2.4. Image processing system

The image processing system for analyzing the drop size consists of a magnifying lens, a CCD camera, an image grabber and a PC computer, as shown in Fig. 4. The magnifying lens consists of a camera bellow and a 19 mm/f3.8 Nikon lens. The Nikon lens was inversely mounted at one end of the bellow and the CCD camera was connected at the other end. When the bellow is stretched out or drawn back, the magnification increases or decreases. The droplet container was mounted on a holder with a two-dimensional advancing mechanism, so that any region in the tray can be picked up for taking a video image. Since droplets are heavier than the collecting liquid, they are all settled down on the floor and can be sharply focused for taking a picture. For a water droplet on a solid surface, the gravity effect makes the droplet deform. When the droplet is in the oil pool, buoyancy force overcomes part of the gravity force and droplet deformation is greatly reduced. Therefore, all the droplets in the oil, even large ones, maintained nearly spherical shape. With a strong lighting from the back through a pin hole, a high-contrast droplet image with a thick halo was recorded, as shown in Fig. 5.

The droplet image was grabbed and digitized by the image grabber, and then processed by the computer. Image processing software was developed for droplet counting and sizing. The high image quality makes the image processing algorithm simpler and more accurate than that for dynamic images taken from flow field [11]. The lens has a magnification up to 11 times, and the image has a spatial resolution up to  $2 \mu\text{m pixel}^{-1}$ . The image screen has a pixel array of  $640 \times 480$ , therefore, droplets of diameter from  $10 \mu\text{m}$  to 1.0 mm can be measured with the full appearance on the screen. If a droplet diameter is larger than 1.0

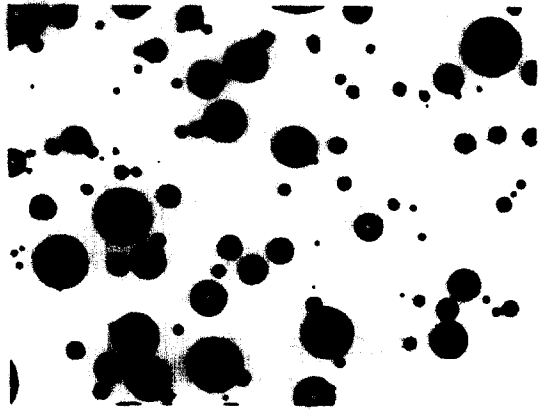


Fig. 5. Digitized droplet image from a water droplet sample.

mm and part of the droplet is cut off by the screen, the droplet diameter is then measured from the curvature of the droplet boundary. The range of droplet size measurement is, therefore, from  $10\ \mu\text{m}$  to 3 mm. If the number density of sampled droplets is high, droplet overlapping may occur. The image software can distinguish the partially overlapping droplets and measure their actual sizes. This is important for measuring large droplet sizes because miscounting of large ones can significantly alter the shape of size distribution due to their large volume. The image processing software can handle hundreds of frames of the digitized images automatically. Thus a large number of droplets can be processed in a relatively short time. The total droplet number in each measurement was over 20 000, therefore the mean droplet size was accurately estimated.

### 3. SOME SAMPLING PROBLEMS AND RECOMMENDED SOLUTIONS

#### 3.1. Droplet deposition inside the probe

Droplet size distribution may change if the drop deposition inside the probe has a preference to certain sizes. Investigations [12–16] have shown that droplets deposit onto the wall mainly by two mechanisms. Droplets with small momentum are strongly affected by the gas turbulent eddies and exhibit random trajectories, and deposition of these droplets is diffusion controlled. Droplets with large momentum are less influenced by turbulence, and they deposit on the wall mainly due to their initial transverse momentum. Jepson *et al.* [16] have experimentally investigated the effect of deposition on droplet size distribution in annular flow. The data showed that the change of the Sauter mean diameter was less than 7% for  $L/D < 20$ , which was comparable to the measurement uncertainty. Although their result indicates that the distortion of drop sizes due to deposition is insignificant for a short probe, the calibration of the system is still necessary.

#### 3.2. Droplet breakup during the capture

In the present system, droplets were collected by an oil film or a pool of immiscible liquid. A question was naturally raised about whether droplet breakup occurred during the collection process. Simple experiments and a qualitative analysis were undertaken to answer this question, and it was concluded that droplet breakup can be effectively prevented if the collection liquid has a smaller surface tension than that of the droplet, a high viscosity and a density similar to that of the droplet.

It is rather difficult to experimentally observe the impingement of small, high-velocity droplets into a liquid surface. Droplet breakup generally obeys certain criteria such as the critical Weber number, therefore, large, low-velocity droplets can be used to conduct the droplet impingement experiment. Droplets of sizes up to 5 mm were produced by liquid dripping from a tube. The droplets were released from different heights so that different droplet velocities were obtained. The maximum height in the laboratory was 5 m and the droplet velocity can reach nearly  $10\ \text{m s}^{-1}$  at the surface of the receiving liquid. Different liquid droplets (water, oil and woods metal drops) and various collection liquids were used in the experiments. By varying the droplet velocity and properties of the receiving liquid (viscosity, surface tension and density), droplet breakup was studied. The following discussion is based on the experimental observations and qualitative analyses.

3.2.1. *Droplet breakup occurs if the surface tension of the droplet is smaller than that of the receiving liquid.* This conclusion was drawn from impingement experiments of heavy manometer oil droplet into water and into molten paraffin. Compared to water, paraffin had a similar viscosity but much smaller surface tension. When the oil droplet was dropped into water, the droplet disintegrated into several small droplets, even if released from a short distance above the surface. When the same droplet was dropped into a pool of molten paraffin, the droplet remained intact. Droplet breakup did not occur even when the droplet was released from a much higher distance. The only significant property difference between water and molten paraffin was the surface tension.

3.2.2. *The density of the collecting liquid should be close to that of the droplet.* If the collection liquid density is too large, the droplet may breakup at the liquid interface. The Taylor instability will occur when a light droplet impinges into a heavier liquid. On the other hand, if the liquid density is too small, the droplet cannot be slowed down effectively. In practice, most common liquids except liquid-metal have similar densities. For heavier liquid-metal droplets, the viscosity of the collection liquid must be high in order to stop droplets in a short distance in the liquid.

3.2.3. *The viscosity of the receiving liquid should be high enough so that droplets can be slowed down rapidly and stopped in a short distance in the liquid.* Experiments revealed that the higher the viscosity of the

receiving liquid was, the less disintegration occurred. In the present system, American Industrial Oil No. 220 (kinematic viscosity is  $2.2 \times 10^{-4} \text{ m}^2 \text{ s}^{-1}$  at  $40^\circ\text{C}$ ) was used for water droplet collection. For heavier woods-metal droplets, much more viscous syrup was used. This phenomena is explained qualitatively as follows: droplet disintegration is the result of a deformation force [17] acting on a droplet for a sufficiently long time. Both the magnitude of the deformation force and the length of force acting time are crucial to droplet breakup. When a droplet travels from air into a liquid, it will be rapidly decelerated due to the drastic change in resisting forces. In such a transient process, the retarding force includes steady drag force, virtual mass force and transient viscous force (Basset force) [18]. The effect due to viscous force is in different orders of magnitude between the high and low viscous fluids. As a result, the time for a drop to slow down below the critical velocity for droplet breakup varies significantly. In the droplet impingement process, the deformation force is so large that only the length of force acting time is the determining factor. When a droplet penetrates into a highly viscous liquid, the droplet velocity is rapidly reduced below the critical velocity for droplet breakup. If this time frame is shorter than the time interval required for droplet deformation leading to the breakup, then droplet disintegration does not occur. When a less viscous liquid is used, the droplet can not be slowed down quickly and it continues to travel in the liquid at a velocity well above the critical velocity for a long time. In this case, the deformation force is large and force acting time is long, therefore, droplet breakup will take place. The use of a high-viscosity fluid is necessary for preventing drop breakup during droplet collection, however, if the viscosity of the fluid is too high, small drops may be suspended in the liquid and never settle down on the bottom. This may cause some difficulties for image analysis.

### 3.3. Droplet coalescence

In order to eliminate the problem of droplet coalescence, the interval of sampling time was controlled to be short so that the droplet number density was low. On the other hand, for an accurate measurement, the number of droplets per sample should be sufficiently high. An optimum time window was selected after several sampling trials. An electrical shutter was installed in the droplet collection box to control the time window. The width of the time window depends on the droplet mass flux. For example, in the experiment of droplet mass flux of  $80 \text{ kg/m}^2\text{s}$  and gas velocity of  $100 \text{ m s}^{-1}$ , a time window of less than  $0.1 \text{ s}$  was used.

## 4. CALIBRATION

Prior discussions showed that droplet breakup and coalescence could be prevented with proper measures. The effect of droplet deposition inside the probe was

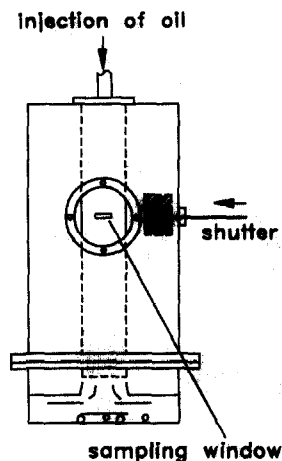
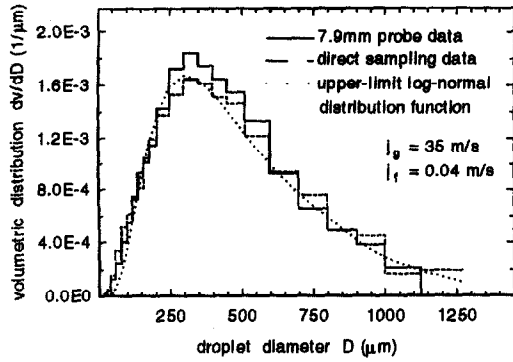


Fig. 6. Droplet collection box used for direct sampling.

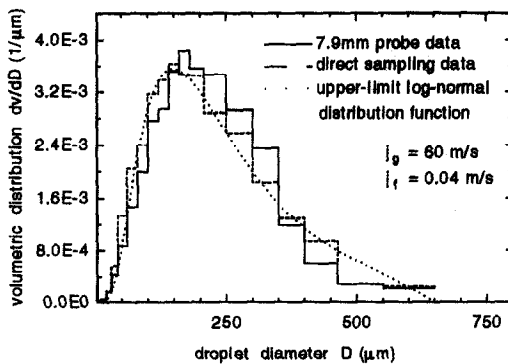
quantitatively evaluated by a calibration method. The procedure included the measurements of droplet size distribution using sampling probes of various sizes and the measurement by a direct sampling. There were two reasons for using this particular calibration method instead of using an optical method. First, the cost of any optical instrument was beyond the budget of this research. Secondly, optical methods are difficult to apply to flow situations with high droplet mass flux and film on the wall.

The first step of the present calibration procedure was to take a clean droplet sample by a direct sampling method. In the direct sampling, the end of the horizontal test section of was fully open and all the droplets across the entire flow area were taken without using a probe. To prevent possible droplet coalescence, only a small fraction of the droplet sample was allowed to enter the collection chamber as shown in Fig. 6 and the interval of sampling time was short. Then, the droplet size distribution was measured, in which the effect of droplet deposition was considered insignificant. The second step was to take droplet samples at the same flow conditions by sampling probes of various sizes and to measure the size distributions. By comparing the droplet size distributions measured by sampling probes with that by the direct sampling, the effect of droplet deposition can be quantitatively examined.

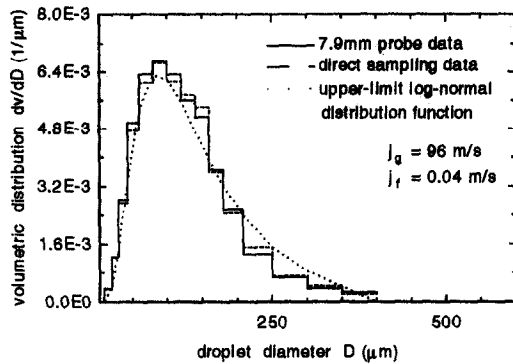
System calibrations were performed at different gas and liquid velocities for different size probes. The calibration results showed that at relatively high gas velocities ( $> 35 \text{ m s}^{-1}$ ), the change in droplet size distribution due to droplet deposition in the probe was insignificant for the  $7.9 \text{ mm}$  i.d. probe ( $L/D = 32$ ) and  $11.1 \text{ mm}$  i.d. probe ( $L/D = 24$ ). Figures 7(a)–(c) show the droplet size distributions from the  $7.9 \text{ mm}$  i.d. probe ( $L/D = 32$ ) at the same liquid velocity but three different gas velocities,  $35$ ,  $60$  and  $96 \text{ m s}^{-1}$ . It can be seen that the size distributions measured by the probe are in a good agreement with the distribution from the direct sampling and the upper-limit log-normal



(a)



(b)



(c)

Fig. 7. Calibration results on droplet size distribution measurement at: (a)  $j_g = 35 \text{ m s}^{-1}$  and  $j_f = 0.04 \text{ m s}^{-1}$ , (b)  $j_g = 60 \text{ m s}^{-1}$  and  $j_f = 0.04 \text{ m s}^{-1}$  and (c)  $j_g = 96 \text{ m s}^{-1}$  and  $j_f = 0.04 \text{ m s}^{-1}$ .

fitting function. The upper limit log-normal distribution function was proposed by Mugele and Evans [19], and given by

$$\frac{dv}{dy} = -\frac{\xi}{\sqrt{\pi}} e^{-(\xi y)^2} \quad (3)$$

$$y = \ln \frac{kD^3}{D_{\max}^3 - D^3} \quad (4)$$

$$k = \frac{D_{\max}^3 - D_{\text{vm}}^3}{D_{\text{vm}}^3} \quad (5)$$

where  $v$ ,  $D$ ,  $D_{\text{vm}}$  and  $D_{\max}$  are the volumetric fraction, droplet diameter, volume median diameter and maximum drop diameter, respectively.  $\xi$  is the distribution parameter which is determined by the experimental data, and  $D_{\max}$  is measured.

The experimental conditions and the measured mean droplet sizes by the probe and direct sampling are shown in Table 1. The comparison shows that the differences between probe measurement and direct sampling are less than 8%, which is comparable to the uncertainties of measurements. The calculated mean droplet volume median diameter by Kataoka and Ishii's model [20] is also listed in Table 1. This model was based on the experimental data from vertical annular flows and given by

$$D_{\text{vm}} = 0.028 \frac{\sigma}{\rho_g j_g^2} Re_f^{-1/6} Re_g^{2/3} \left( \frac{\rho_g}{\rho_f} \right)^{-1/3} \left( \frac{\mu_g}{\mu_f} \right)^{2/3} \quad (6)$$

Since there was no reliable correlation or sufficient database for horizontal annular droplet flow, it was still meaningful to use this correlation to predict the mean drop size, particularly at high gas velocity where the gravitational effect becomes unimportant. The good agreement between the measurements and model predictions also demonstrated the reliable performance of the present system. It was found in the experiment that, at much lower gas velocities (below  $20 \text{ m s}^{-1}$ ), deposition of large drops in the probe was significant. However, good measurements were obtained at high gas velocities ( $> 35 \text{ m s}^{-1}$ ). The present system is particularly suitable for droplet size measurement at high gas velocities.

## 5. MEASUREMENT RESULTS IN APPLICATION

The present system has been successfully used for droplet size measurement in a transient droplet flow system, Direct Containment Heating test facility. DCH is a postulated scenario after a nuclear reactor core meltdown accident and it is an important safety problem for the light water reactors. In the DCH scenario, a significant amount of molten core materials are ejected out of the failed reactor vessel and entrained by the high-velocity blowdown steam. The mass fraction of entrainment and droplet size distribution are the crucial factors governing the heat transfer to the containment atmosphere and the pressurization of containment. In order to obtain the experimental data and to have a good understanding of droplet entrainment and dispersion process, a DCH facility with a 1/10 linear scale of the reactor system was built to simulate the accident. The present system has been used to measure the droplet size distribution and droplet mass flux in the simulation experiments. The details of the facility were given in ref. [21]. The configuration of the facility and the set-up of the droplet sampling system are shown in Fig. 8. Two kinds of liquids, air and woods-metal, were used to simulate the molten reactor core, and air was used

Table 1. The comparison of mean drop sizes among measurements by sampling probes, measurements by direct sampling and model calculation

$j_f$ [m s <sup>-1</sup> ]	$j_g$ [m s <sup>-1</sup> ]	Measurement by 7.9 mm probe			Measurement by direct sampling			Model
		$D_{32}$	$D_{vm}$ [ $\mu\text{m}$ ]	$D_{max}$	$D_{32}$	$D_{vm}$ [ $\mu\text{m}$ ]	$D_{max}$	$D_{vm}$ [ $\mu\text{m}$ ]
0.04	35.0	345	440	1200	350	460	1300	425
0.04	60.0	177	220	650	167	215	650	207
0.04	93.0	96	126	400	94	123	400	110

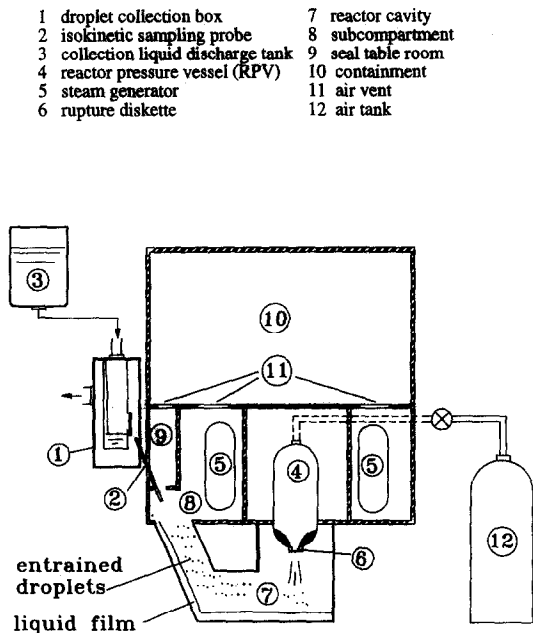
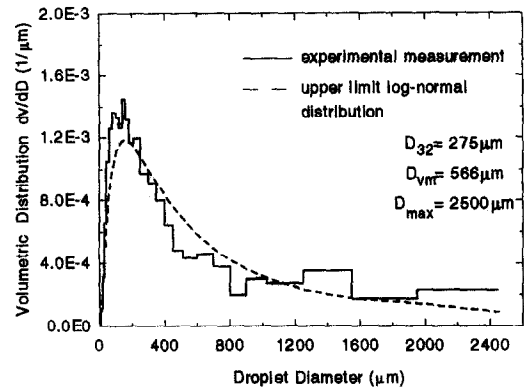


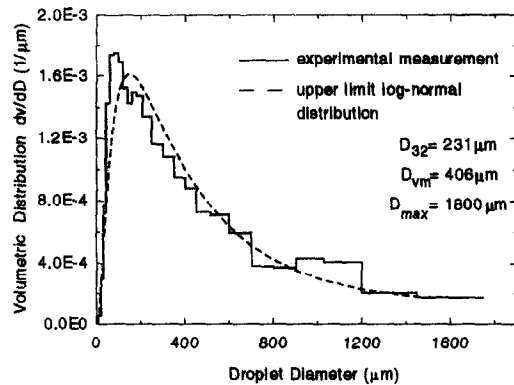
Fig. 8. Droplet sampling system used in Purdue Direct Containment Heating Facility.

to simulate steam. The liquid was charged into the RPV (reactor pressure vessel), and the RPV was pressurized by actuating the solenoid valve. The rupture disk broke at a specific pressure level and the liquid was then discharged into the reactor cavity. After the completion of the liquid discharge, air began to blow down. The liquid in the cavity was entrained by the gas stream and carried into the subcompartment, and part of the entrained mass dispersed into the containment atmosphere. Three isokinetic sampling probes were mounted above the exit of cavity for droplet sampling. The probes were aligned parallel to the gas stream in the cavity chute in order to minimize droplet deposition in the probe.

Figures 9(a)–(b) show the measured droplet size distributions at different time window in air–water simulation tests. These data show that droplet sizes are relatively large at the beginning of entrainment and become smaller later on. This trend of change is consistent with the physical process of entrainment. The spread of the droplet size distribution is wider than that in the steady state due to the change in gas velocity during the transient. Figure 10 shows the size distribution of woods–metal droplet. The woods–



(a)



(b)

Fig. 9. Droplet size distribution measurements in transient DCH air–water experiment: (a) time window 1; (b) time window 2.

metal droplets were captured in a pool of syrup and the temperature of syrup was below woods–metal melting point (70°C). Since woods–metal droplets were quickly solidified in the liquid pool, droplet coalescence was insignificant. Therefore, the time window for sampling was selected to be much wider to cover the whole entrainment time interval. These experimental measurements provided a valuable database for evaluating the containment performance in such a severe accident scenario.

## 6. CONCLUSIONS

Droplet size measurements become rather difficult under some restrictive experimental conditions in two-



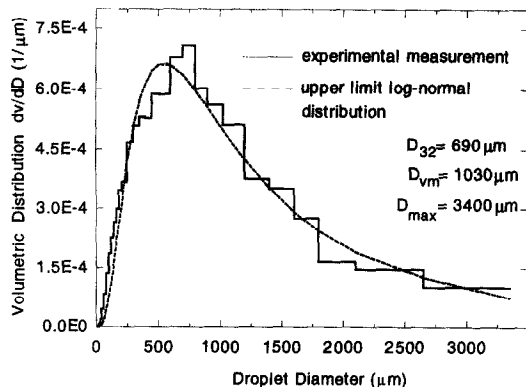


Fig. 10. Size distribution of liquid-metal droplets measured in the air-liquid metal experiment.

phase flow, such as high-transient process, high droplet flux, existence of liquid film on the wall and non-transparent liquid (liquid-metal) droplets. A novel system was developed to perform droplet size measurements under these difficult conditions. Some concerns associated with the system such as droplet deposition, breakup and coalescence were addressed and answers and practical solutions were provided. The system was calibrated by a direct sampling method, and the reliability of its performance was also examined by the comparison between measurements and model predictions. Experiments showed that the present system was particularly suitable for high-velocity gas-droplet flows. The application of the system to a nuclear reactor severe accident simulation experiment has demonstrated its usefulness to highly complicated systems under transient conditions.

*Acknowledgements*—The authors would like to express their sincere appreciation to Dr S. T. Revankar of the School of Nuclear Engineering and Professor J. P. Sullivan of the School of Aeronautics and Astronautics at Purdue University for their constructive comments and suggestions, and also to Dr R. Y. Lee of U.S. NRC for his valuable discussions and support to this research. This work was performed under the auspices of the U.S. Nuclear Regulatory Commission.

#### REFERENCES

1. R. Henry, An evaluation of fission product release rates during debris dispersal, *Proceedings of ANS Int. Topical Meeting—Probability, Reliability and Safety Assessment*, Vol. 1, p. 375 (1989).
2. A. H. Lefebvre, *Atomization and Sprays*, p. 380. Hemisphere, New York (1989).
3. B. J. Azzopardi, Measurement of drop sizes, *Int. J. Heat Mass Transfer* **22**, 1245–1279 (1979).
4. M. Wicks and A. E. Dukler, *In situ* measurements of drop size distribution in two-phase flow, *Int. Heat Transfer Conf.*, Chicago (1966).
5. L. E. Gill, G. F. Hewitt, J. W. Hitchon and P. M. C. Lacey, Sampling probe studies of the gas core in annular two-phase flow, *Chem. Engng Sci.* **18**, 525–535 (1963).
6. T. Allen, *Particle Size Measurement* (3rd Edn), p. 54. Chapman and Hall, New York (1981).
7. N. Adorni, I. Casagrande, L. Cravarolo, A. Hassid and M. Silvestri, Experimental data on two-phase adiabatic flow: liquid film thickness, phase and velocity distribution, pressure drops in vertical gas-liquid flow, CISE R-35, Centro Informazioni Studi Esperienze, Milano, Italy (1961).
8. F. A. Schraub, Isokinetic sampling probe technique applied to two-component, two-phase flow, GEAP-5287, General Electric, San Jose, California (1966).
9. S. V. Paras and A. J. Karabelas, Droplet entrainment and deposition in horizontal annular flow, *Int. J. Multiphase Flow* **17**, 455–468 (1991).
10. K. V. L. Rao, Liquid nitrogen cooled sampling probe for the measurement of spray drop size distribution in moving liquid-air sprays, presented at 1st *Int. Conf. on Liquid Atomization and Spray Systems*, Tokyo, Japan (1978).
11. E. Fantini, L. Tognotti and A. Tonazzini, Drop size distribution in sprays by image processing, *Comput. Chem. Engng* **14**, 1201–1211 (1990).
12. P. W. James, G. F. Hewitt and P. B. Whalley, Droplet motion in two-phase flow, AERE-R 97, Atomic Energy Research Establishment, Harwell, Berkshire, U.K. (1980).
13. P. Hutchinson, G. F. Hewitt and A. E. Dukler, Deposition of liquid or solid dispersion from turbulent gas stream: a stochastic model, *Chem. Engng Sci.* **26**, 419–439 (1971).
14. E. N. Ganic and K. Mastanaiah, Investigation of droplet dispersion from a turbulent gas stream, *Int. J. Multiphase Flow* **7**, 401–422 (1981).
15. M. M. Lee, T. J. Hanratty and R. J. Adrian, The interpretation of droplet motion measurements with a diffusion model, *Int. J. Multiphase Flow* **15**, 459–469 (1989).
16. D. M. Jepsen, B. J. Azzopardi and P. B. Whalley, The effect of gas properties on drops in annular flow, *Int. J. Multiphase Flow* **15**, 327–339 (1989).
17. M. Ishii and K. Mishima, Two-fluid model and hydrodynamic constitutive relations, *Nucl. Engng Des.* **82**, 107–126 (1984).
18. A. B. Basset, *A Treatise on Hydrodynamics*, Vol. 2, p. 285. Deighton, Bell and Co, Cambridge (1888).
19. R. A. Mugele and H. D. Evans, Droplet size distribution in sprays, *Ind. Engng Chem.* **43**, 1317–1324 (1951).
20. I. Kataoka, M. Ishii and K. Mishima, Generation and size distribution of droplet in annular two-phase flow, *J. Fluids Engng* **105**, 230–238 (1983).
21. M. Ishii, S. T. Revankar, G. J. Zhang, Q. Wu and P. O'Brien, Separate effects studies on phenomena of corium dispersion in direct containment heating, presented at 21st *Water Reactor Safety Information Meeting*, Upton, New York (1993).